

Periodic striations on beryllium and tungsten surfaces by indirect femtosecond laser irradiation

C. P. Lungu, C. M. Ticoș,^{a)} C. Poroșnicu, I. Jepu, M. Lungu, A. Marcu, C. Luculescu, G. Cojocaru, D. Ursescu, R. Bănici, and G. R. Ungureanu

National Institute for Laser, Plasma and Radiation Physics, 077125 Bucharest, Romania

(Received 20 October 2013; accepted 27 February 2014; published online 11 March 2014)

Femtosecond laser pulses with $\lambda = 800$ nm were focused in air at one atmosphere and in deuterium (D) at low pressure. Submicron periodic structures were observed on surfaces made of Be, W and a mixture of Be-W immersed in these gases and placed nearly parallel with the laser beam, at $300 \mu\text{m}$ from the focal spot. In air, no structures were observed on Be. For the Be-W mixture, the periodic structures were uniform and parallel when formed in D but irregular in air. In this last case the striations were organized into small patches of 1 to $2 \mu\text{m}$ in size. © 2014 AIP Publishing LLC. [<http://dx.doi.org/10.1063/1.4868241>]

The quest for finding materials which can withstand high heat fluxes and resist to bombardment of ionized particles, neutrons and photons is a key topic in fusion technology. Be and W are so far among the best candidates and are already used for building the first wall or the divertor of tokamaks.¹ Each of these materials has advantages and disadvantages. While Be is a low Z material and has less potential to contaminate with impurities the hot magnetically confined plasma, W has a low sputtering rate, a low absorption rate of D and T and a high melting temperature. The need to understand the behavior of these materials under extreme conditions of temperatures and particle fluxes is of paramount importance for designing and building the future large fusion machines such as ITER.² Testing of these materials has been conducted at several facilities by recreating at best the conditions present in a fusion plasma.^{3,4}

Layers of Be and W qualitatively compatible with fusion technology can be deposited on different substrates using a thermionic vacuum arc plasma.^{5,6} Here, a heated filament installed at the cathode produces an electron beam which is focused on a small piece of the metal which will be coated (e.g., Be, W, etc.) and located at the anode. After intense electron bombardment the metal at the anode heats up until it melts and eventually it vaporizes. By applying a high voltage between the anode and cathode a bright plasma is formed in the vapors of the metal which is further deposited on a substrate positioned close enough to the electrodes.⁷

In this Letter, we report on the results of exposing coatings made of Be, W, and a mixture of Be-W to a plasma formed in D and air by focusing high power ultrashort laser pulses. The gas breakdown was possible due to the high laser intensity obtained in the focal spot. Surprisingly, we observed the appearance of periodic striations after firing a relatively large number of laser pulses, between 30 and 300. Periodic structures are routinely observed when the laser beam is aimed directly at the surface. Here however the laser beam is approximately parallel to the surface, as shown in Fig. 1(a). The craters created by the plasma on the surfaces and shown in Fig. 1(b) were imaged with a scanning electron microscope

(SEM). Their shape is elongated, in accordance with the propagation direction of the beam. Their size clearly depends on the number of laser pulses: more pulses lead to the formation of larger craters. The samples were produced in-house by coating thin rectangular chips with a size 12×15 mm and made of high density graphite with Be and W using the thermionic vacuum arc.⁵⁻⁷ The coatings had a good uniformity and thickness of about $2 \mu\text{m}$. For the sample containing both Be and W, the weight percentage was $\simeq 50\%$ – 50% .

Laser induced periodic surface structures (LIPSSs) were intensely investigated lately. They were produced by direct laser irradiation on different metals such as Au and Pt,⁸ Al,⁹ stainless steel and Ni,¹⁰ Ti and Mo,¹¹ and W.¹²⁻¹⁵ Besides metals, LIPSS were observed on semiconductors.¹⁶ In most reports the laser had $\lambda = 800$ nm and the width of the

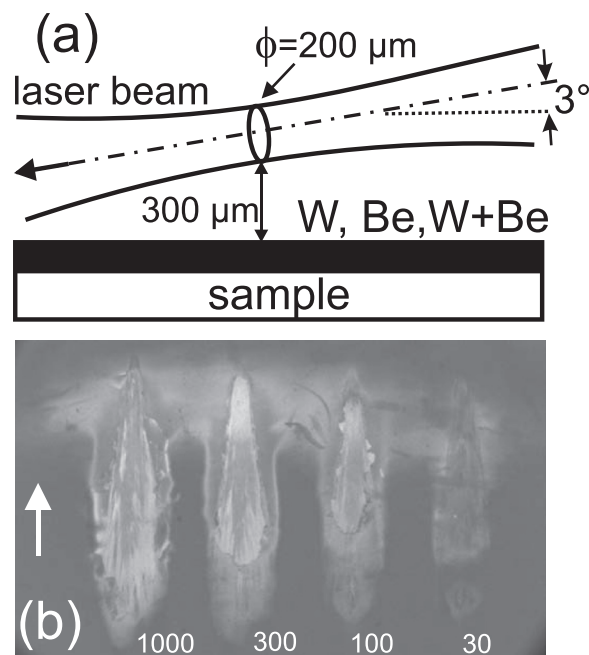


FIG. 1. (a) The laser beam is focused in a spot with diameter ϕ near the samples coated with Be, W, and a mixture of W-Be; (b) SEM images of craters on the Be surface produced in air after firing 10^3 , 300, 100, and 30 laser pulses, respectively. The arrow indicates the laser beam direction.

^{a)}Electronic mail: catalin.ticos@inflpr.ro

structures varied between tens and hundreds of nanometers depending on the number of laser pulses and fluence which was changed in a wide range from 0.07 J/cm^2 (Refs. 11 and 12) to 0.16 J/cm^2 (Ref. 10) and from 2.5 to 7 J/cm^2 .^{13,14}

Irradiation of the gas near the samples was carried out with single and multiple laser pulses using the 17 TW Ti-Sapphire system called TEWALAS. The laser system employs the chirped pulse amplification technique for delivering ultra-short pulses. The laser pulses had the following parameters: duration 70 fs, energy per pulse 6 mJ, repetition rate 10 Hz and p polarization. The laser beam was focused by a plane-convex lens with 300 mm focal length. The lens was made of fused silica and antireflex coated for an optimum broadband between 700 nm and 900 nm. Its diameter was 75 mm while the incident laser beam had 18 mm at FWHM. The spatial profile of the laser beam was Gaussian. The diameter of the focusing spot was about $200 \mu\text{m}$ resulting in a laser fluence of 19.1 J/cm^2 . The beam made a 3° angle with the surface of the samples and was focused in their vicinity inside the gas, at a distance of $300 \mu\text{m}$ from the surface, as shown in Fig. 1(a). The laser beam propagated in vacuum from the compressor to the samples which were inserted in a small target chamber provided with viewports. The samples were mounted on a movable mechanical support which could be adjusted in the horizontal plane and along a vertical direction. The role of the target chamber was twofold in the experiments: first it allowed the immersion of the sample in different gases at a controlled pressure (including vacuum) and secondly it contained the debris resulted from the interaction of the produced laser-plasma with the surfaces. The Be dust is known to be a health hazard. The experiments were carried out in air at atmospheric pressure and in D at 20 Torr. D was chosen to simulate a tokamak plasma.

The exposed samples of Be and W to air plasma are shown in Fig. 2. In Figs. 2(a)–2(c), we can observe the lamellar pattern of the Be surface consisting in overlapped stacks of a few hundreds of nm in size. This structure is typical for Be coatings obtained by vapor deposition or by plasma arc. This initial structure starts to change morphology in c) and takes a granular aspect in d). The average size of a granule is in the tens of nanometers range. Due to the prolonged exposure to laser-produced plasma (i.e., over 300 shots) the granulation becomes more dense and eventually melts forming small droplets at the top of a fiber-like network, in Fig. 2(f). No sign of surface arrangement is seen at any time during the shots. W has a more homogeneous aspect after 1 or 10 shots, as seen in Figs. 2(g) and 2(h). A pattern of elongated structures starts to emerge after 30 shots shown in Fig. 2(i). This pattern evolves into a clear and well delimited periodic structure shown in Figs. 2(k) and 2(l). The surface looks as if composed of aligned rod-shaped structures of hundred of nanometers or even $1 \mu\text{m}$ in length. The average spatial periodicity is $\Lambda = 400 \text{ nm}$ and 270 nm after 300 and 10^3 shots, respectively.

The situation is somehow different in D for both metals. For Be, after 1 shot the sample surface has small granules, of a few nanometers in size, in Fig. 3(a). After 100 shots, a pattern with rather wide irregular striations is observed on the surface, as shown in Fig. 3(d). The average spacing between the striations is $\Lambda \approx 330 \text{ nm}$. After 300 shots, the striations are

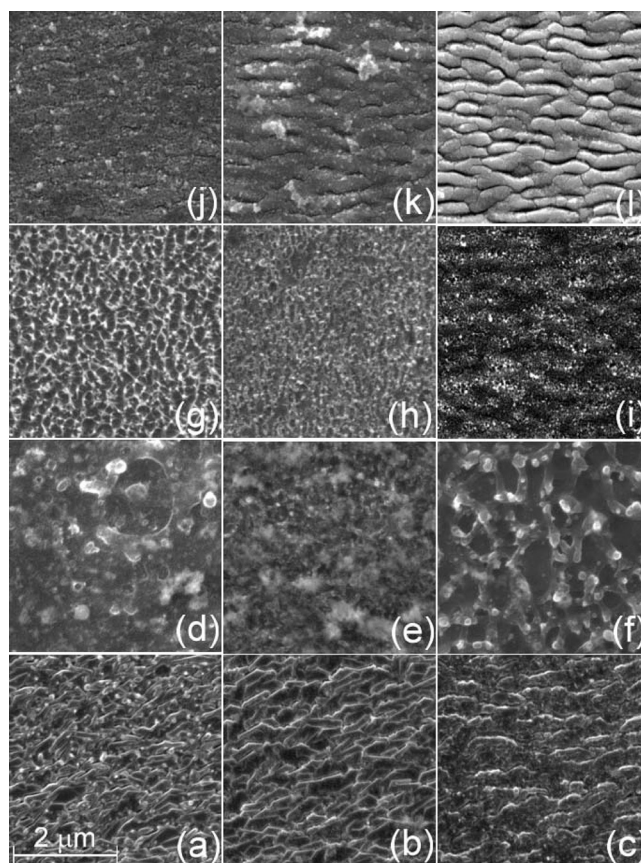


FIG. 2. Exposed Be samples in (a) to (f) and W samples in (g) to (l) in air at atmospheric pressure after 1, 10, 30, 100, 300, and 1000 shots, respectively.

replaced by large granules which eventually melt and become more homogeneous after 1000 shots, in Figs. 3(e) and 3(f), respectively. In the case of W immersed in D, only after about 300 shots a pattern of striations becomes clearly visible with $\Lambda = 360 \text{ nm}$, as seen in Fig. 3(k). The striations become narrower in Fig. 3(l), where $\Lambda = 290 \text{ nm}$, after 1000 shots.

The most interesting situation is seen in the case of samples containing the mixture Be-W. In air after 1 to 30 shots the surface is dominated by large micron size particles, as shown in Figs. 4(a)–4(c). In Fig. 4(c), the microparticles are covered with nanometer size protuberances, probably because of the surface melting. After 100 shots, these large microparticles have a tendency of organization into planar strips, as presented in Figs. 4(d) and 4(e). The formation of periodic structure is more visible after 1000 shots where stacks of 5 to 10 elongated microparticles are well delimited by wide and deep trenches. The average spatial periodicity is $\Lambda = 400 \text{ nm}$ after 300 shots and remains the same after 10^3 shots.

An example of how the periodicity Λ has been inferred is presented in Fig. 5. Here, Fig. 5(a) shows the spatial two-dimensional Fourier transform (2-d FT) of the surface made of Be-W exposed to 30 shots of D plasma. The first pair of dominant peaks excepting the origin in Fig. 5(b) clearly shows a cyclic pattern with $\Lambda = 370 \text{ nm}$.

The experimental findings demonstrate that the formation of striations depends on the type of material, the ambient gas and the number of laser shots. It appears that D is a more favorable gas than air as demonstrated by Fig. 3(d), which shows Be striations, compared to its analogous Fig. 2(d)

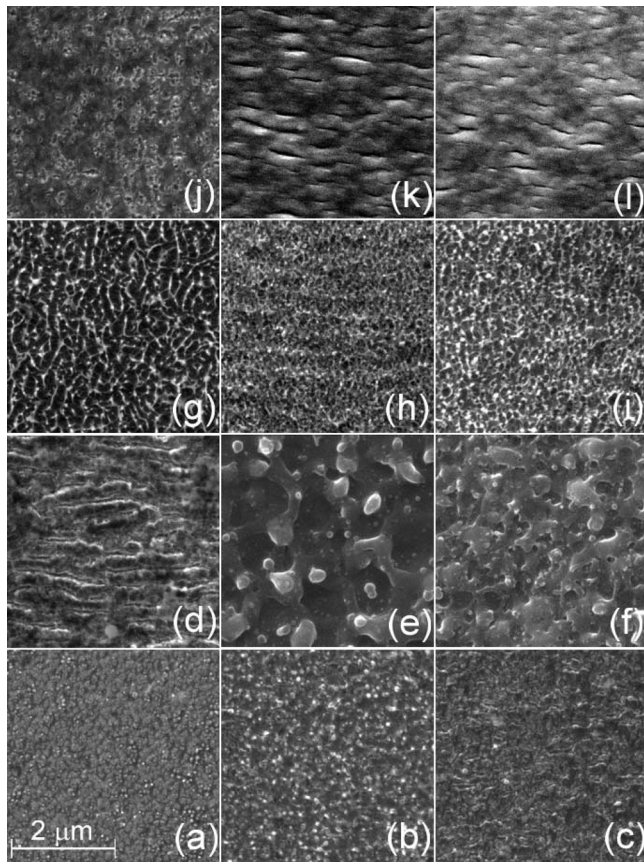


FIG. 3. Exposed Be samples in (a) to (f) and W samples in (g) to (l) in D at 20 Torr after 1, 10, 30, 100, 300, and 1000 shots, respectively.

where no surface periodicity can be observed. Furthermore, in the case of W clearly defined striations are observed after 300 shots in D compared to 1000 shots in air, as seen in Figs. 3(k) and 2(i), respectively. Concerning the surface made of the Be-W mixture the striations are perfectly aligned and parallel after only 30 shots in D, as seen in Figs. 4(i) and 4(j), compared to the results obtained in air shown in Figs. 4(c) and 4(d). An important observation is that Λ decreases with the number of laser shots for W in air and D, and for the composite Be-W in D, keeping the other parameters unchanged. In the case of the Be-W samples exposed in air, once the periodic structures were formed Λ did not vary with the number of laser shots, at least in the limit set by our experiment of 10^3 shots.

The morphology of the analyzed striations is similar to that observed in experiments which used a laser beam incident on a W target.^{12,14,15} Vorobyev and Guo¹² reported a period $\Lambda = 289$ nm in air at $\lambda = 400$ nm and a fluence of 0.35 J/cm², while at $\lambda = 800$ nm the period depended on the number of laser shots: $\Lambda = 560$ nm after 40 shots and 470 nm after 800 shots, respectively, at a fluence of 0.44 J/cm², concluding that $\Lambda \geq \lambda/2$. In our case, the laser beam does not hit the sample surface and the measured period is in the range $\Lambda = 290$ nm to 400 nm for both W and Be, thus $\Lambda \leq \lambda/2$. On the other hand, ripples with periodicity $\Lambda = 30$ to 100 nm $\ll \lambda = 800$ nm were observed for a higher fluence of 3 J/cm² and after 10 shots.¹³

Several mechanisms for producing striations by indirect laser irradiation are being analyzed. For the laser parameters,

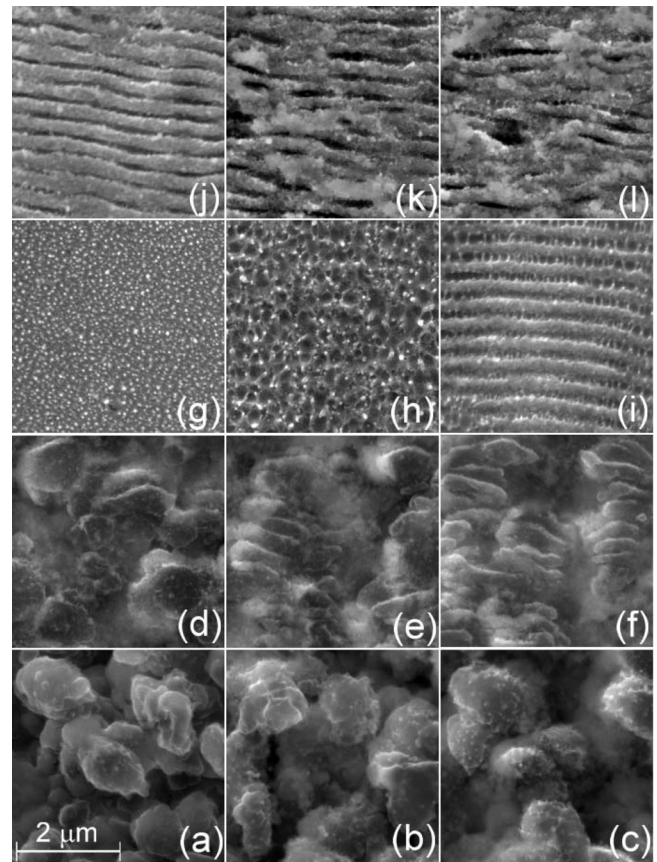


FIG. 4. Exposed samples made of Be-W mixture in air in (a) to (f) and in D in (g) to (l), after 1, 10, 30, 100, 300, and 1000 shots, respectively.

we infer a power density of $\approx 5 \times 10^{14}$ W/cm². The laser power $P_{las} = 86$ GW is well above the Kerr-induced filamentation threshold in air $P_{Kerr} = 1.9$ GW.¹⁷ At the same time $P_{las} \ll P_{rel}$, where $P_{rel} \approx 17 (\omega/\omega_p)$ [GW]¹⁸ is the relativistic self-focusing threshold, ω is the laser frequency and ω_p is the plasma frequency. The possibility that the striations could be produced by the plasma waves created in gas and impinging on the surface is ruled out since $\lambda_p(\mu\text{m}) \approx 3.3 \times 10^{10} n_e(\text{cm}^{-3})^{-1/2}$, where λ_p is the wavelength of plasma waves and n_e is the electron density of plasma. For the laser fluence and power density of our experiment, we expect $n_e \ll 10^{18}$ cm⁻³ resulting in $\lambda_p \gg 1$ μm . Another scenario is that the laser light is scattered off the plasma towards the surface. The laser pulse can be subjected to Raman or Brillouin

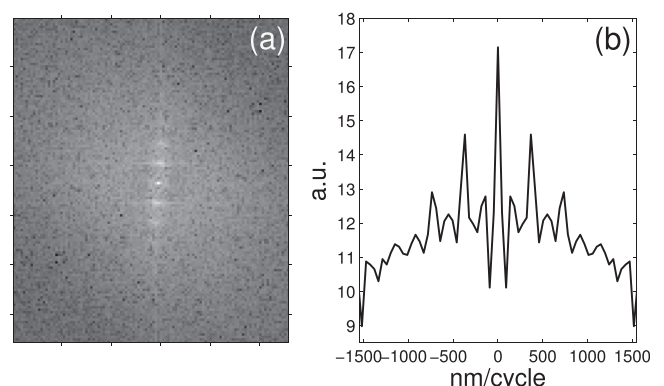


FIG. 5. (a) 2-d FT of the image shown in Fig. 4(i) and (b) spatial periodicity of striations.

instabilities and side-scattered at large angles relative to the incident direction. However, the growth times calculated for the conditions of our experiment are $\simeq 10^{-12}$ s and $\simeq 10^{-11}$ s for the two cases,^{18,19} respectively, thus a few orders of magnitude longer than the pulse duration. Finally, it has been shown that filamentation of a short laser pulse in air can lead to conical emission and a spectral angular dispersion due to nonlinear frequency conversion in the formed plasma.^{17,20} Moreover, while conical emission is weaker than the filament core, it can contain a fraction (in the tens of percents) of the incident beam energy.²¹ A fraction of 10% of the incident laser pulse would correspond to about 1.9 J/s. If we consider the solid angle 0.4π of the irradiated area ($\approx 4 \times 10^4 \mu\text{m}^2$) relative to a uniform energy distribution in 2π , then the fluence of $\simeq 0.38$ J is in agreement with previous reports of direct irradiation.¹²

The mechanism for surface striations can be explained as the result of interference between the incident laser beam and the surface plasmons although neither Be and nor W have the real part of the dielectric permittivity negative: $\varepsilon_W = 5.22 + i19.44$ (Ref. 22) and $\varepsilon_{Be} = 2.7 + i2.8$ (Ref. 23) at $\lambda = 800$ nm. Other factors such as surface roughness and transfer of heat from the plasma to the surface during the ripple formation have to be accounted for.²⁴

In conclusion, striations were observed on the surface of samples made of Be, W and a mixture of Be-W immersed in air at atmospheric pressure and in D at 20 Torr after exposure to plasma created by focusing a high power ultrashort laser pulses within the nearby gas, at $300 \mu\text{m}$ from the surfaces. The morphology of the surface structures is similar to that observed in experiments with direct laser irradiation of the surfaces. For a coating made of Be-W, the striations were localized within areas of 1 to $2 \mu\text{m}$ well delimited from each other. This observation could be of interest for the creation of surfaces with variable morphology at the micron level in which periodic structures alternate with regions with no particular structuring.

This work was supported by a grant of the Romanian National Authority for Scientific Research, CNCS—UEFISCDI, Project No. PN-II-ID-PCE-2011-3-0522.

- ¹C. Thomser, V. Bailescu, S. Brezinsek, J. W. Coenen, H. Greuner, T. Hirai, J. Linke, C. P. Lungu, H. Maier, G. Matthews, Ph. Mertens, R. Neu, V. Philipps, V. Riccardo, M. Rubel, C. Ruset, A. Schmidt, I. Uytendhouwen, and JET EFDA Contributors, *Fusion Sci. Technol.* **62**(1), 1 (2012), available at http://www.ans.org/pubs/journals/fst/a_14103.
- ²R. A. Pitts, S. Carpentier, F. Escourbiac, T. Hirai, V. Komarov, A. S. Kukushkin, S. Ligo, A. Loarte, M. Merola, R. Mitteau, A. R. Raffray, M. Shimada, and P. C. Stangeby, *J. Nucl. Mater.* **415**(Suppl. 1), S957 (2011).
- ³A. Schmidt, T. Hirai, S. Keusemann, M. Rödig, G. Pintsuk, J. Linke, H. Maier, V. Riccardo, G. F. Matthews, M. Hill, and H. Altmann, *Phys. Scr.* **T138**, 014034 (2009).
- ⁴H. Greuner, B. Boeswirth, J. Boscary, and P. McNeely, *J. Nucl. Mater.* **367–370**(Pt. B), 1444 (2007).
- ⁵C. P. Lungu, I. Mustata, V. Zoroschi, A. M. Lungu, A. Anghel, P. Chiru, M. Rubel, P. Coad, and G. F. Matthews, *Phys. Scr.* **T128**, 157 (2007).
- ⁶A. Marcu, C. M. Ticos, C. Grigoriu, I. Jepu, C. Porosnicu, A. M. Lungu, and C. P. Lungu, *Thin Solid Films* **519**, 4074 (2011).
- ⁷C. P. Lungu, A. Marcu, C. Porosnicu, I. Jepu, J. Kovac, and V. Nemanic, *IEEE Trans. Plasma Sci.* **40**, 3546 (2012).
- ⁸A. Y. Vorobyev, V. S. Makin, and C. Guo, *J. Appl. Phys.* **101**, 034903 (2007).
- ⁹E. V. Golosov, A. A. Ionin, Yu. R. Kolobov, S. I. Kudryashov, A. E. Ligachev, S. V. Makarov, Yu. N. Novoselov, L. V. Seleznev, and D. V. Sinitsyn, *Nanotechnol. Russia* **6**, 237 (2011).
- ¹⁰J.-W. Yao, C.-Y. Zhang, H.-Y. Liu, Q.-F. Dai, L.-J. Wu, S. Lan, A. V. Gopal, V. A. Trofimov, and T. M. Lysak, *Opt. Express* **20**, 905 (2012).
- ¹¹M. Hashida, Y. Ikuta, Y. Miyasaka, S. Tokita, and S. Sakabe, *Appl. Phys. Lett.* **102**, 174106 (2013).
- ¹²A. Y. Vorobyev and C. Guo, *J. Appl. Phys.* **104**, 063523 (2008).
- ¹³Q.-Z. Zhao, S. Malzer, and L.-J. Wang, *Opt. Express* **15**, 15741 (2007).
- ¹⁴Q.-Z. Zhao, S. Malzer, and L. J. Wang, *Opt. Lett.* **32**, 1932 (2007).
- ¹⁵L. Xue, J. Yang, Y. Yang, Y. Wang, and X. Zhu, *Appl. Phys. A: Mater. Sci. Process.* **109**, 357 (2012).
- ¹⁶J. Bonse, J. Krüger, S. Höhm, and A. Rosenfeld, *J. Laser Appl.* **24**, 042006 (2012).
- ¹⁷D. Faccio, M. A. Porras, A. Dubietis, G. Tamošauskas, E. Kučinskas, A. Couairon, and P. D. Trapani, *Opt. Commun.* **265**, 672 (2006).
- ¹⁸T. M. Antonsen and P. Mora, *Phys. Fluids B* **5**, 1440 (1993).
- ¹⁹H. A. Baldis, E. M. Campbell, and W. L. Kruer, "Laser-plasma interactions," in *Handbook of Plasma Physics*, edited by M. N. Rosenbluth and R. Z. Sagdeev, Volume 3 of *Physics of Laser Plasma*, edited by A. M. Rubenchik and S. Witkowski (Elsevier, New York, 1991), p. 409.
- ²⁰O. G. Kosareva, V. P. Kandidov, A. Brodeur, C. Y. Chien, and S. L. Chin, *Opt. Lett.* **22**, 1332 (1997).
- ²¹A. Couairon and A. Mysyrowicz, *Self-focusing: Past and Present, Topics in Applied Physics* (Springer, New-York, 2009), Vol. 114, p. 297.
- ²²D. W. Lynch and W. R. Hunter, *Handbook of Optical Constants of Solids* (Academic, New York, 1985), p. 357.
- ²³W. J. Tropf, T. J. Harris, and M. E. Thomas, in *Electro-Optics Handbook*, edited by R. W. Waynant and M. N. Ediger (McGraw-Hill, New York, 2000), p. 411.
- ²⁴A. Y. Vorobyev and C. Guo, *Opt. Express* **14**, 13113 (2006).